Analysis of Differences from Nuclear Data Library in NaCl-KCl-UCl3 MSR Core Design: ENDF/B-VII.1 versus JENDL-5

Yubin Go [a], Seong Jun Yoon [a], Jae Uk Seo [a], Sung-Kyun Zee [a], Tongkyu Park [a*]
a FNC Technology Co., Ltd, 13 Heungdeok 1-ro, Giheung-gu, Yongin-si, 16954, Korea
*Corresponding author: tongkyu@fnctech.com

Keywords : Molten Salt Reactor, Nuclear Data, JENDL-5, ENDF/B-VII.1, K-39, Sensitivity Analysis

1. Introduction

A maritime long-term fast-spectrum molten salt reactor (MSR) core design is being developed by FNC [4,5]. The design objective is a thermal power of 100 MWth with a core lifetime of 22.5 effective full power years (EFPY) without refueling. The fuel salt is a NaCl-KCl-UCl3 ternary composition (mole fraction 43.3:21.7:35.0, 19.75 w/o HALEU, chlorine enriched to 99 a/o in Cl-37), and all criticality and depletion calculations are performed using the Monte Carlo transport code OpenMC 0.15.3 [1], with ENDF/B-VII.1 [3] as the baseline evaluated nuclear data library.

Figures 1 (X-Y plane) and 2 (X-Z plane) depict the present core configuration, while Table I summarizes the key specifications. Control drums in the MgO reflector regulate reactivity in the fast-spectrum design of the core.

The choice of the evaluated nuclear data library affects design margins such the excess reactivity, shutdown margin, and critical control-drum rotation angle. Therefore, it is important to quantify the magnitude and source of the discrepancy before finalizing the design. Specifically, the current design uses a ternary composition with KCl (average temperature: 580 °C, density: 3.22 g/cm³), which results in a high in-core potassium loading; potassium makes up 5.2% of the fuel salt by mass and 8.0% of the fuel salt by atom fraction.

In this study, the difference in core characteristics between ENDF/B-VII.1 and JENDL-5 [2] is evaluated on an identical model under identical conditions, and the discrepancy

is decomposed successively at the element, isotope, and reaction-type levels to identify its origin.

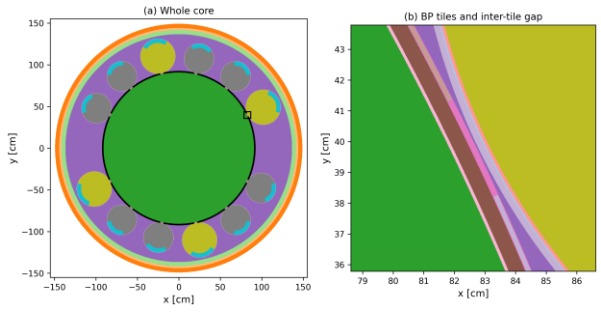


Fig. 1. X-Y plane views of the reference core model (green: fuel salt; purple: MgO reflector; gray/olive: control/shutdown drums; cyan: B4C absorber pads; orange/light green: vessel and outer structural layers): (a) whole core at z = 19 cm, where the black arcs mark the thin burnable-poison (BP) shell and its 12 inter-tile gaps aligned with the drum azimuths (thickness exaggerated for visibility); (b) close-up of a BP inter-tile gap at a drum azimuth (z = 19 cm; the dark band is the B4C BP tile inside the thin shell, interrupted at the gap).

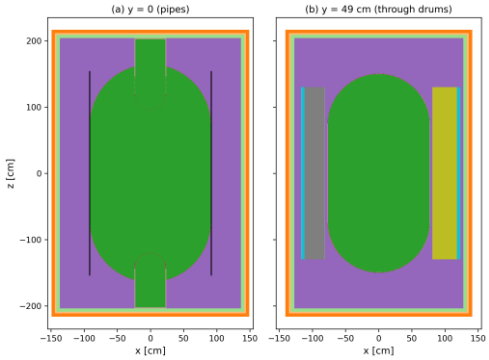


Fig. 2. X-Z plane views of the reference core model: (a) section through the inlet/outlet pipes (y = 0); (b) section through the centers of a control drum (left) and a shutdown drum (right) (y = 49 cm).

Table I. Core Specification

Parameter	Value	Material/Note
Thermal power	100 MWth	—
Design cycle length	22.5 EFPY	No refueling
Fuel salt	NaCl-KCl-UCl3 (43.3:21.7:35.0)	19.75 w/o HALEU
Chlorine enrichment	Cl-37 99 a/o	—
Reflector	MgO	—
Reactivity control	Reflector control drums	—
Spectrum	Fast	—
Code / library	OpenMC 0.15.3	ENDF/B-VII.1

2. Methods and Results

The library comparison was performed on an identical model under the same conditions. All calculations used the all-drums-out (ADO) configuration at a fuel-salt temperature of 580 °C with an identical random number seed. 500,000 particles per batch with 400 total batches (100 inactive) provided a statistical uncertainty of about ±6 pcm on the reactivity of each calculation (about ±8

pcm on a difference between two calculations). Since JENDL-5 does not provide an evaluation for natural carbon, the corresponding entries were substituted by C-12 and C-13 based on their natural abundances. For the decomposition, hybrid libraries were constructed by replacing the entries of selected nuclides, or of selected reaction types (channels) within the K-39 evaluation, of the ENDF/B-VII.1 library with the corresponding JENDL-5 data, so that each substitution isolates a single contribution; only the inelastic-scattering entry is an approximation, in which the ENDF/B-VII.1 partial inelastic cross sections are scaled to the JENDL-5 magnitude while the level structure and secondary-energy distributions remain unchanged. To resolve the non-potassium remainder, the other constituents were likewise substituted independently in five groups — Na, Cl, U, the MgO reflector (Mg, O), and the structural and absorber materials (45 nuclides); natural carbon was left unchanged in these substitutions because JENDL-5 provides no evaluation for it. The effective delayed neutron fraction β_eff was evaluated with the iterated fission probability (IFP) method.

2.1 Library-to-Library Difference

Table II compares the core features calculated using the two libraries.

Table II. Core characteristics with the two libraries

Library	**keff**	**ρ [pcm]**	**β_eff [pcm]**
ENDF/B-VII.1	1.01490 ± 0.00006	+1469	718.5 ± 2.9
JENDL-5	1.02029 ± 0.00006	+1989	714.6 ± 2.8
Difference	+0.00539	+520 ± 8 (66σ)	−3.9 ± 4.0

A difference in reactivity of 520 ± 8 pcm, between the two libraries is statistically notable at the level of 66σ. In contrast, the difference in β_{eff} is −3.9 ± 4.0 pcm, statistically insignificant, and the neutron generation time Λ varies only from 10.71 μs to 10.27 μs (−0.44 μs, about −4 %), indicating that the kinetics parameters are insensitive to the library choice. This consistency aligns with neutron absorption data being the source of the difference, rather than fission or delayed neutron data.

2.2 Element- and Isotope-Level Decomposition

To identify the nuclides responsible for the difference, a hybrid library was constructed, wherein only the potassium data from the fuel salt were substituted with the JENDL-5 data, and the identical calculation was repeated (Table III). The potassium substitution yields +383 ± 8 pcm, accounting for about 74 % of the total difference. The remaining +138 ± 8 pcm was not obtained from a separate calculation; it is the arithmetic residual of the total difference minus the potassium contribution. To resolve the concern that this residual might conceal mutually cancelling contributions, each remaining constituent group was substituted independently in the same manner as potassium: chlorine, uranium, sodium, the MgO reflector, and the structural and absorber materials (Table III). The substitutions yield +87 ± 8 pcm for chlorine, +78 ± 8 pcm for uranium, +22 ± 9 pcm for the structural and absorber materials, +12 ± 8 pcm for sodium, and −27 ± 8 pcm for the MgO reflector. Their sum, +172 ± 19 pcm, agrees with the residual within 1.7σ; the remainder is attributable to natural carbon, for which JENDL-5 provides no evaluation, and to the non-additivity of independent substitutions. No single non-potassium constituent exceeds 90 pcm and the only negative contribution is small, so the residual does not conceal large mutually cancelling terms. Thus, despite the fact that the fuel is a chloride salt, potassium dominates over chlorine, whose contribution is about a quarter of that of potassium. At the isotope level, replacing the entire K-39 data set yields +399 ± 8 pcm and the K-41 contribution is −17 ± 9 pcm as a residual, indicating that the potassium effect is primarily due to the single nuclide K-39.

Table III. Element-, isotope-, and constituent-level substitution effects

Substitution	**Δρ [pcm]**	**Note**
All nuclides (JENDL-5)	+520 ± 8	Total difference
K (all isotopes)	+383 ± 8	About 74 % of total
K-39	+399 ± 8	Essentially the whole potassium effect
K-41	−17 ± 9	Derived residual (K minus K-39)
Non-K remainder	+138 ± 8	Derived residual (total minus K); resolved below
Cl (Cl-35, Cl-37)	+87 ± 8	Largest non-K term
U (U-235, U-238)	+78 ± 8	
Structural and absorber materials	+22 ± 9	Natural carbon excluded
Na-23	+12 ± 8	Statistically insignificant
MgO reflector (Mg, O)	−27 ± 8	Only negative term
Sum of the five non-K groups	+172 ± 19	Consistent with the remainder (-35 ± 20, 1.7σ)

2.3 Reaction-Type Attribution

The initial hypothesis examined was the difference in radiate capture (n, γ) cross section for K-39. However, the K-39 capture cross sections for the two libraries are nearly identical below 1 MeV (a difference of about 0.1 mb), and substituting the capture reaction alone yields +8 ± 8 pcm, which is statistically insignificant. The capture data are therefore excluded as the origin.

The primary source involves the charged-particle emission absorption reactions (n,p) and (n,α) in the fast energy range. In these reactions, K-39 absorbs a neutron and emits either a proton or an alpha particle, respectively. Both reactions are exothermic (Q = +0.22 and +1.36 MeV), but the emitted charged particle must pass through the Coulomb barrier, therefore cross sections are extremely small at low energies and only become significant above roughly 1 MeV. Figures 3 and 4 compare the K-39 (n,p) and (n,α) cross sections of the two libraries over the full energy range. In the region above about 1 MeV where the cross sections become significant, ENDF/B-VII.1 evaluates both reactions higher than JENDL-5, and since the fast core spectrum extends into this region, the evaluation difference translates into a reactivity difference. Weighted by the fuel-salt spectrum of the reference calculation, 90 % of the resulting reaction-rate difference arises between 1.2 and 4.0 MeV for (n,p) and between 2.0 and 7.0 MeV for (n,α) (shaded bands in Figs. 3 and 4); in these intervals ENDF/B-VII.1 exceeds JENDL-5 by up to about 85 mb and 150 mb, respectively, whereas the low-energy tails, where the two evaluations differ qualitatively, contribute less than 2 %. Both reactions are parasitic absorption that removes neutrons from the system, so keff calculated with ENDF/B-VII.1, which evaluates these cross sections higher, is lower; indeed, substituting only these two absorption reactions yields +426 ± 8 pcm, which by itself accounts for the entire K-39 effect of +399 ± 8 pcm.

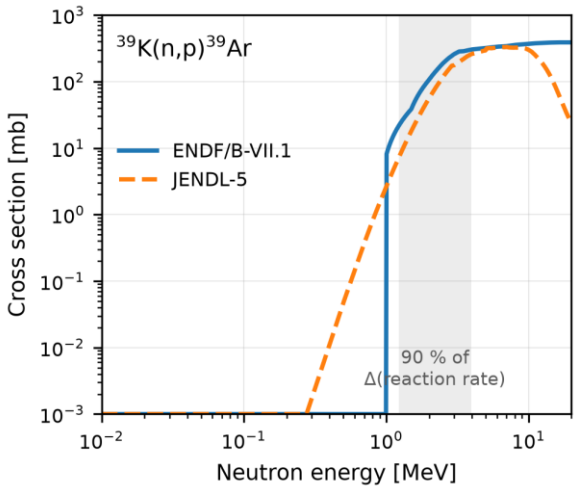


Fig. 3. K-39 (n,p) cross sections of ENDF/B-VII.1 and JENDL-5. The shaded band marks the energy interval (1.2–4.0 MeV) containing 90 % of the difference in the fuel-salt reaction rate between the two libraries, evaluated with the 47-group fuel spectrum of the reference calculation.

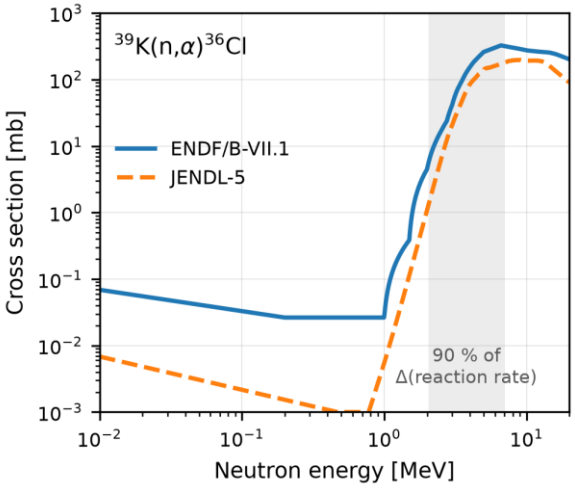


Fig. 4. K-39 (n,α) cross sections of ENDF/B-VII.1 and JENDL-5. The shaded band marks the energy interval (2.0–7.0 MeV) containing 90 % of the difference in the fuel-salt reaction rate between the two libraries, evaluated as in Fig. 3.

The completeness of the decomposition was confirmed by summing the contributions of the individual reaction types (Table IV). The sum of charged-particle absorption (+426 ± 8), radiative capture (+8 ± 8), elastic scattering (+12 ± 8), and inelastic scattering (−12 ± 8) is +435 ± 25 pcm, which agrees within statistics with the +399 ± 8 pcm obtained by replacing the entire K-39 data set (difference +35 ± 21 pcm, 1.6σ); the quoted uncertainties account for the correlation introduced by the common ENDF/B-VII.1 reference calculation. This implies the entire difference is accounted for without any overlooked reaction type. The inelastic contribution is statistically insignificant; its ratio-scaled entry captures the cross-section magnitude effect only. Possible artifacts of the cross-section processing were also examined and excluded: both libraries were processed onto the same temperature grid, and neither evaluation carries unresolved-resonance data for K-39.

Table IV. Reaction-type-isolated substitution effects for K-39

Substituted reaction type	**Δρ [pcm]**	**Note**
All K-39 data	+399 ± 8	Essentially the whole potassium effect
Charged-particle absorption (n,p)+(n,α)	+426 ± 8	Dominant contribution
Capture (n,γ)	+8 ± 8	Statistically insignificant
Elastic scattering	+12 ± 8	Statistically insignificant

Inelastic scattering	−12 ± 8	Ratio-scaled approximation; insignificant
Sum of reaction types	+435 ± 25	Consistent with full K-39 substitution (+35 ± 21)

3. Conclusions

The reactivity difference between ENDF/B-VII.1 and JENDL-5, +520 ± 8 pcm, was evaluated on an identical model under identical conditions. Its origin was traced via a three-step decomposition at the element, isotope, and reaction-type levels. The majority of the difference is concentrated in a single nuclide and a single group of reactions — the fast (n,p)/(n,α) charged-particle emission absorption of K-39 (+426 pcm). The sum of the contributions of the individual reaction types (+435 ± 25 pcm) agrees with the full K-39 substitution effect (+399 ± 8 pcm), confirming the completeness of the decomposition. The non-potassium contribution of about +138 pcm was resolved by independent substitution into chlorine (+87 pcm), uranium (+78 pcm), the structural and absorber materials (+22 pcm), sodium (+12 pcm), and the MgO reflector (−27 pcm), with no large cancelling terms; the radiative capture reaction is statistically insignificant, and the kinetics parameters β_{eff} and Λ are insensitive to the library choice.

These findings show that the library choice shifts the excess reactivity by about 500 pcm, and they provide a quantitative basis for treating this shift as an uncertainty item to be considered in the criticality and reactivity-margin evaluations of the present core design and of similar potassium-bearing chloride fast cores. In order to systematically identify the various contributors to the operational uncertainty of the MSR design, we intend to evaluate the depletion reactivity with a spatially resolved burnable-poison consumption history, as well as the effective delayed neutron fraction and its reactivity effect considering delayed neutron precursor transport by the fuel-salt flow.

ACKNOWLEDGMENTS

This work was supported by the National Research Foundation of Korea (NRF) grant funded by the Korea government (MSIT) (RS-2023-00260898).

REFERENCES

[1] P.K. Romano, N.E. Horelik, B.R. Herman, A.G. Nelson, B. Forget, K. Smith, "OpenMC: A State-of-the-Art Monte Carlo Code for Research and Development," Annals of Nuclear Energy, Vol. 82, pp. 90-97 (2015).
[2] O. Iwamoto et al., "Japanese Evaluated Nuclear Data Library Version 5: JENDL-5," Journal of Nuclear Science and Technology, Vol. 60, No. 1, pp. 1-60 (2023).
[3] M.B. Chadwick et al., "ENDF/B-VII.1 Nuclear Data for Science and Technology: Cross Sections, Covariances, Fission Product Yields and Decay Data," Nuclear Data Sheets, Vol. 112, No. 12, pp. 2887-2996 (2011).
[4] Y. Go, T. Park, S.K. Zee, J.U. Seo, S.J. Yoon, "Conceptual core design study of a maritime molten salt fast reactor," Annals of Nuclear Energy, Vol. 222, 111571 (2025).
[5] Y. Go, S.J. Yoon, J.U. Seo, S.K. Zee, T. Park, "Comparative Depletion Analysis of a Marine Molten Salt Fast Reactor Considering Explicit Primary Loop Geometry," Trans. of KNS Spring Mtg., Jeju, Korea, May 7-8, 2026.